


Geophysical Research Letters[®]



RESEARCH LETTER

10.1029/2022GL100911

Greenland Ice Sheet Ice Slab Expansion and Thickening

N. Jullien¹ , A. J. Tedstone¹ , H. Machguth¹, N. B. Karlsson² , and V. Helm³ 

Key Points:

- Ice slabs were already present in the early 2000s in southwest, central-west and north Greenland
- Ice slabs expanded inland from 2002 to 2018 and thickened by accretion to both their tops and undersides
- Near-surface ice layers support subsequent ice slab development

Supporting Information:

Supporting Information may be found in the online version of this article.

Correspondence to:

N. Jullien,
nicolas.jullien@unifr.ch

Citation:

Jullien, N., Tedstone, A. J., Machguth, H., Karlsson, N. B., & Helm, V. (2023). Greenland ice sheet ice slab expansion and thickening. *Geophysical Research Letters*, 50, e2022GL100911. <https://doi.org/10.1029/2022GL100911>

Received 19 AUG 2022

Accepted 25 APR 2023

Author Contributions:

Data curation: N. Jullien, N. B. Karlsson

Formal analysis: N. Jullien

Methodology: N. Jullien, A. J. Tedstone, H. Machguth, V. Helm

Writing – original draft: N. Jullien, A. J. Tedstone

Writing – review & editing: N. Jullien, A. J. Tedstone

¹Department of Geosciences, University of Fribourg, Fribourg, Switzerland, ²Geological Survey of Denmark and Greenland, Copenhagen, Denmark, ³Alfred Wegener Institute, Helmholtz Centre for Polar and Marine Sciences, Bremerhaven, Germany

Abstract We use airborne accumulation radar data acquired over the Greenland Ice Sheet between 2002 and 2018 to identify changes in ice slab extent and thickness. We show that ice slabs several meters thick were already present at least as early as 2002. Between 2012 and 2018, they expanded by 13,400–17,600 km² inland, or 37%–44%. Our results document that the extremely warm summer of 2012 produced near-surface ice layers at higher elevations, enabling ice slabs to develop with only moderate melting in the following summers. With repeat flights along a transect in southwest Greenland, we show that moderate melting primarily causes slab thickening through uniform accretion on top of the ice slabs, while large melting events can also trigger localized accretion below existing ice slabs.

Plain Language Summary Above the equilibrium line elevation, seasonal snow is not entirely removed by summer melting. As a result, firn—an interannual layer made of old snow and refrozen meltwater—builds up. Firn holds the potential to buffer sea level rise by trapping liquid water within its pore space. However, surface melting has increased in recent decades, making large quantities of water available to percolate into the firn where it refreezes, eventually creating meters-thick ice slabs that hinder future percolation. We mapped ice slabs in the subsurface firn (0–20 m depth) by using airborne radar surveys and show that they have expanded inland and thickened from 2002 to 2018. Once formed, ice slabs continue to thicken, even under moderate melt conditions. Recent increases in the area drained by surface rivers on the ice sheet match well with the ice slabs extent, so we conclude that ice slabs will be an important control on the future runoff area of the ice sheet.

1. Introduction

In the 1990s, the mass balance of the Greenland Ice Sheet (GrIS) was close to equilibrium, but has been negative for the last two decades (The IMBIE Team, 2020). Iceberg calving rates have increased (King et al., 2020; Rignot et al., 2008; The IMBIE Team, 2020) and the surface mass balance has decreased as a result of increasing melt and runoff (Enderlin et al., 2014; Fettweis et al., 2017; The IMBIE Team, 2020; van den Broeke et al., 2016). Furthermore, extremely warm summers such as in 2010, 2012, 2016, and 2019 (Mikkelsen et al., 2016; Tedesco & Fettweis, 2020; Tedesco et al., 2011, 2013) triggered unprecedented surface melt rates at high elevations (Hall et al., 2013; Nghiem et al., 2012) and exceptionally high runoff volumes (van Angelen et al., 2014; Mikkelsen et al., 2016).

Recent increases in surface melting have densified the subsurface firn (Machguth et al., 2016; Mikkelsen et al., 2016; van Angelen et al., 2014). Firn is found above the equilibrium line and consists of interannual snow-pack, the density of which increases by compaction through burial but also due to percolation and refreezing of surface meltwater (Braithwaite et al., 1994; Brown et al., 2011; Pfeffer & Humphrey, 1998). Firn has the potential to trap and store meltwater within its pore space, thereby buffering the GrIS contribution to sea level rise (Harper et al., 2012; Pfeffer et al., 1991).

In the percolation zone, where surface melt rates are substantial but usually do not deplete the seasonal snow completely, the fate of meltwater varies mainly with annual snowfall. Where snowfall rates are high (~1,000 ± 400 mm w.e. per year), mostly in southeast and south Greenland, liquid water percolates to a depth where it forms perennial firn aquifers (Forster et al., 2014; Miège et al., 2016; Miller et al., 2022). Conversely, in regions where accumulation rates are lower and which have recently experienced significant melting, ice slabs several meters thick can form—mostly along the west, north and northeast of the GrIS (MacFerrin et al., 2019; Miller et al., 2022). In these regions, increased meltwater percolation during several successive summers fused centimeters-scale ice lenses into increasingly contiguous ice layers tens of centimeters thick and eventually

© 2023. The Authors.

This is an open access article under the terms of the [Creative Commons Attribution License](https://creativecommons.org/licenses/by/4.0/), which permits use, distribution and reproduction in any medium, provided the original work is properly cited.

meters-thick slabs, decreasing the firn's permeability (de la Peña et al., 2015; Vandecrux et al., 2019). Ice slabs form an aquitard, preventing most subsequent meltwater from reaching the relict pore space below (MacFerrin et al., 2019; Machguth et al., 2016).

Ice slabs favor the development of surface streams in the high percolation zone (Machguth et al., 2016; Mikkelsen et al., 2016). The area of the ice sheet drained by surface rivers increased by 29% between 1985 and 2020, corresponding strongly with the locations of ice slabs mapped previously and suggesting that 5%–10% of recent ice-sheet-wide mass losses originated from these newly densified parts of the accumulation zone (Tedstone & Machguth, 2022). This underlines that it is essential to understand firn densification and ice slab development for inclusion in ice sheet mass balance models that are used for projections of ice sheet runoff (de la Peña et al., 2015). Despite their emerging importance to future runoff magnitude, ice slabs have only been mapped over a short time period: with accumulation radar from 2010 to 2014 (MacFerrin et al., 2019), and through a proxy approach with satellite microwave radiometry from 2015 to 2019 (Miller et al., 2022). Here we investigate changes in the extent and thickness of ice slabs using airborne radar observations acquired during spring-time campaigns between 2002 and 2018.

2. Data and Methods

To map ice layer and slab locations in 2002–2003 we used radargrams collected by 600–900 MHz accumulation radar (Kanagaratnam et al., 2004; Lewis, 2010). To examine changing ice thickness during 2010–2018, we used 550–900 MHz accumulation radar (Carl et al., 2023; CReSIS, 2021; Rodriguez-Morales et al., 2010); the 2010–2014 source data are the same as in MacFerrin et al. (2019). Both datasets were collected during spring before melting began.

Data acquired during 2002–2003 have virtually no radiometric information because the provider (CReSIS, 2021) detrended the data in the logarithmic domain (J. Paden, pers. comm. 2020). We therefore identified ice presence and order-of-magnitude thickness in these radargrams by manual expert interpretation. See Text S1 in Supporting Information S1 for more information.

For radargrams acquired between 2010 and 2018, we developed a semi-automated approach based on MacFerrin et al. (2019) to derive changes in ice thickness through time in the uppermost 20 m of the firn. MacFerrin et al. (2019) calculated normalized thresholds specific to each individual radargram to quantify ice thickness. When we compared repeat radargrams over successive years processed with this method, we found unrealistic differences in ice thickness. Here, we therefore use ice presence identified from in-situ ground penetrating radar measurements by MacFerrin et al. (2019) to manually identify ice presence in a coincident accumulation radar overflight. From this overflight, we derived the signal strength distribution associated with ice presence. The signal strength of ice partially overlaps with the signal strength distribution of the surrounding porous firn. Following a sensitivity analysis, we identified lower and upper signal strength thresholds which yield the minimum and maximum likely ice presence, respectively. We used these thresholds to determine ice presence in all other radargrams acquired between 2010 and 2018. In the subsequent analysis we use the maximum likely ice presence unless specified otherwise. We classify areas as “ice slabs” where radar-detected ice is at least 1 m thick and consider the maximum retrievable thickness to be 16 m. “Ice layers” refer to ice less than ~1 m thick. Full details of the methods are in Text S2 in Supporting Information S1.

As a proxy for surface melting, we calculated annual Positive Degree Hour sums using a similar approach to degree-day modeling (Hock, 2003), using in-situ 2 m air temperatures from the automatic weather station KAN_U (Fausto et al., 2021). We summed all positive hourly average temperatures each year.

3. Results

3.1. Ice Slab Expansion From 2002 to 2018

In the 2002–2003 radargrams, ice slabs (Figures 1a and 1b) could be readily distinguished from other characteristic sub-surface features. Radar returns in the ablation zone (Figure 1c) are generally uniform with no major variations in signal strength. The percolation zone exhibits thin and sharp layering probably associated with decimeter-scale ice layers (Figure 1d), and layers several meters thick indicative of ice slabs (Figure 1e). The dry snow zone shows regular parallel layering associated with annual snow accumulation (Figure 1f).

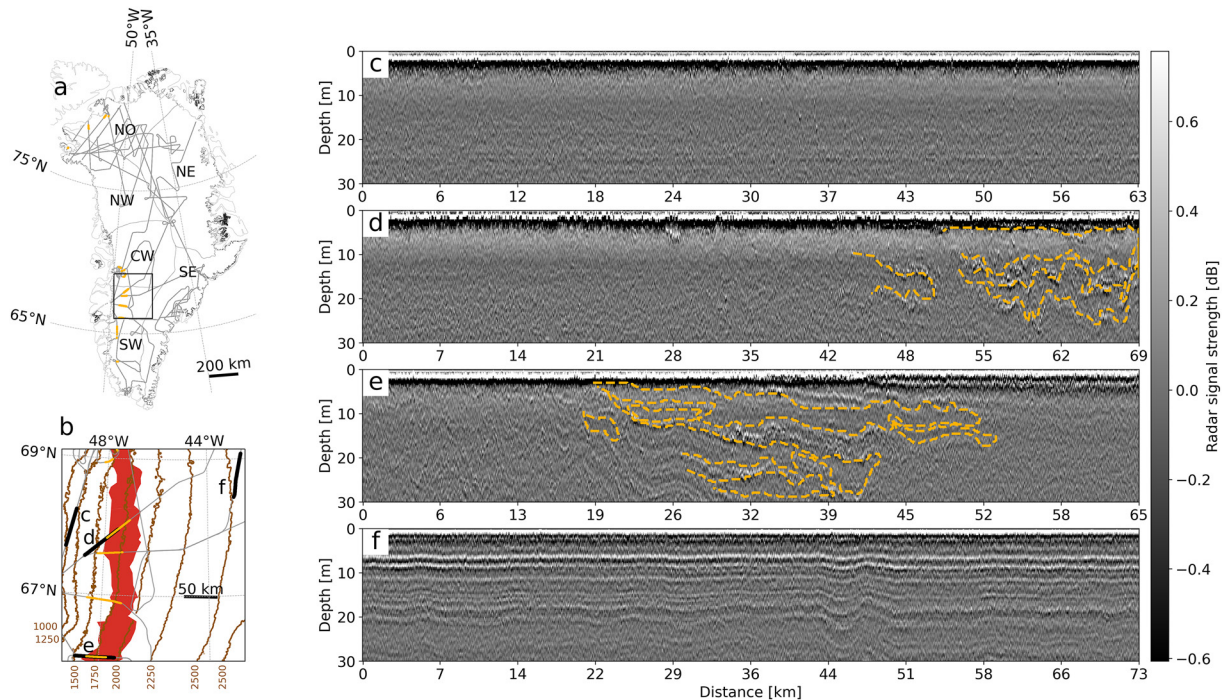


Figure 1. Ice layers and slabs in central and southwest Greenland in 2002–2003. (a) Greenland-wide 2002–2003 flight lines (gray), ice layers and slabs (orange). (b) Overview of radargram locations (black lines), 2002–2003 ice layers and slabs (orange), 2010–2018 ice slabs extent (red), elevation contours (brown). Radargrams with ice layers/slabs identification overlaid (orange dashed lines) acquired from the (c) ablation zone (d–e) percolation zone and (f) dry snow zone.

We found ice slabs up to several meters thick in SW Greenland (Figures 1b, 1d, and 1e). Although the observations are relatively sparse, ice slabs were also identified in the CW, in the vicinity of Sermeq Kujalleq’s (Jakobshavn Isbrae) high percolation zone. Ice layers and slabs were identified in the NO but not in the NW nor the NE, although spatial coverage was limited in the latter regions (Figure 1a).

By 2018, ice slabs occupied 60,400–73,500 km² (minimum and maximum estimates respectively), consistent with indirect ice slab retrievals from satellite microwave radiometry extending over 76,000 km² in 2015–2019 (Miller et al. (2022)). Except in the southern part of SW Greenland, we did not identify any regions with entirely new ice slabs in either 2002–2003 or 2017–2018 compared to the 2010–2014 mapping performed by MacFerrin et al. (2019).

We estimate that the ice slab area increased from 2010–2012 to 2017–2018 by 37% in the NE and the SW, 48% in the NW, and 54% in the CW (Figure 2a). We calculated the highest ice slab elevation in each period by picking the highest elevation in 10 km-wide boxes, then calculating the median value in each region. The increase in area was primarily driven by ice slab expansion to higher elevations along the west margin (Figure 2b), in agreement with the upslope expansion of ice slabs identified by Miller et al. (2022).

3.2. Ice Slab Thickening

The accumulation radar used between 2010 and 2018 has a vertical resolution of 65 cm in snow and firn (Rodríguez-Morales et al., 2014), enabling us to examine ice slab thickness changes along six transects named A–F (locations shown in Figure 2a). By considering initial ice slab thickness and subsequent thickening through time, we classified up to three stages of ice slab development on each transect: “well developed,” “in development,” and “initiation.”

The “well-developed” stage corresponds to regions where the ice slab was already at least 10 m thick at the start of the studied period and showed little or no evidence of further thickening. On transect F, median ice thickness stayed roughly the same in 2017 compared to 2010 (Figures 3b and 3c). Considering all transects except B, there was a median thickening of 0.7 m, reaching a median thickness of 14 m (Table S3 in Supporting Information S1).

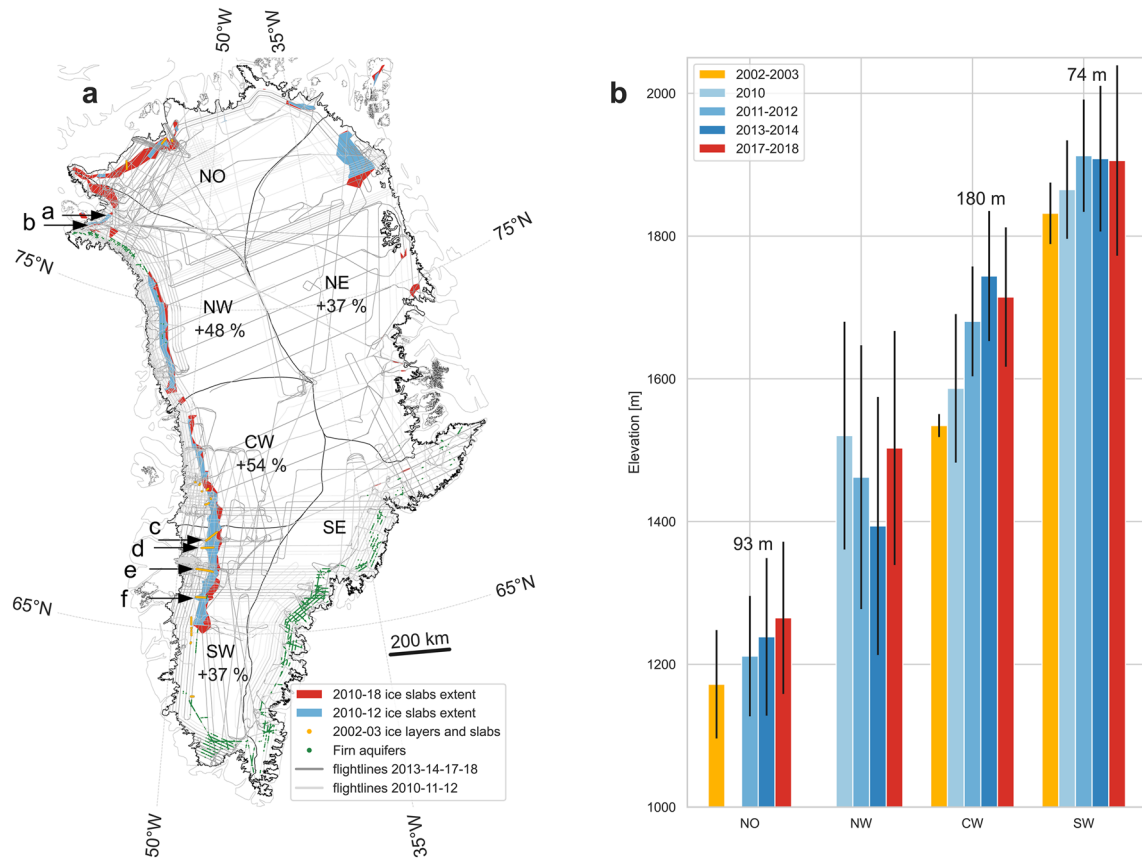


Figure 2. Maximum ice slab extent from 2002 to 2018. (a) Ice layers and slabs in 2002–2003 (orange), ice slab extent in 2010–2012 (blue) and 2010–2018 (red), firn aquifers in 2010–2014 (Miège et al., 2016) (green). Accumulation radar flight lines (light gray: 2010–2012, dark gray: 2013–2018). Percentages indicate the expansion of ice slab extent in 2010–2018 with respect to 2010–2012. Black arrows indicate the transects introduced in Section 3.2. (b) Highest ice slab elevation ± 1 standard deviation (black bars) in each region. Numbers indicate the change in highest ice slab elevation between 2002–2003 and 2017–2018. Elevations are above WGS84 ellipsoid. Elevation changes in the NE are omitted, as well as extent change in the NO and north of the NW as there was insufficient overlap in flight lines between the different periods (see Figures S6a–S6e in Supporting Information S1).

In the “development” stage, ice slabs thickened by several meters. Median thickness on transect F increased from 4.2 to 11.5 m, equivalent to an increase of 191% from 2010 to 2017 (Figures 3d and 3e). Across all six transects, all slabs in “development” thickened, by a median of 61% (Table S3 in Supporting Information S1).

Finally, in the “initiation” stage, the firn was free of ice slabs at the start of the study period, but had new ice slabs by 2017. On transect F, a new ice slab developed above ~ 1930 m with a median thickness of 5 m by 2017 (Figures 3f and 3g). Similar initiation was also observed on transects B–E, with new ice slabs having a median thickness of 5.5 m by 2017/18 (Table S3 in Supporting Information S1).

We examined ice slab initiation and thickening in more detail along transect E, near to the KAN_U weather station at which meteorological measurements have been made continuously since 2009. This transect offers repeat radargrams acquired in 2012, 2013, and 2018, plus radargrams in 2014 and 2017 that are offset by a few hundred meters (Figures 4a e.g. 900 m at 3.8 km, 1,770 m at 20 km). Ice thickness can vary significantly between radargrams which do not overlap perfectly. For example, there is $\sim 59\%$ less ice between 3.8 and 5.6 km in 2014 retrieval compared to 2013 (Figures 4b and 4c). Nonetheless, we still identified overall thickening between 2012 and 2018, by 9% from 10 km further downstream (not shown) to 3.8 km and by 43% between 3.8 and 7.7 km (Figure 4d). A new ice slab developed beyond 8.5 km.

We observed that ice slabs can thicken by substantial localized ice accretion beneath the slab, and by widespread ice accretion on top of the slab. Accretion beneath existing slabs creates distinct “ice blobs” at depth relative to the surrounding slab. On our transects, these “ice blobs” generally spread laterally over several tens of meters rather than several kilometres in the NW as observed by Culberg et al. (2022). For instance, between 3.8 and

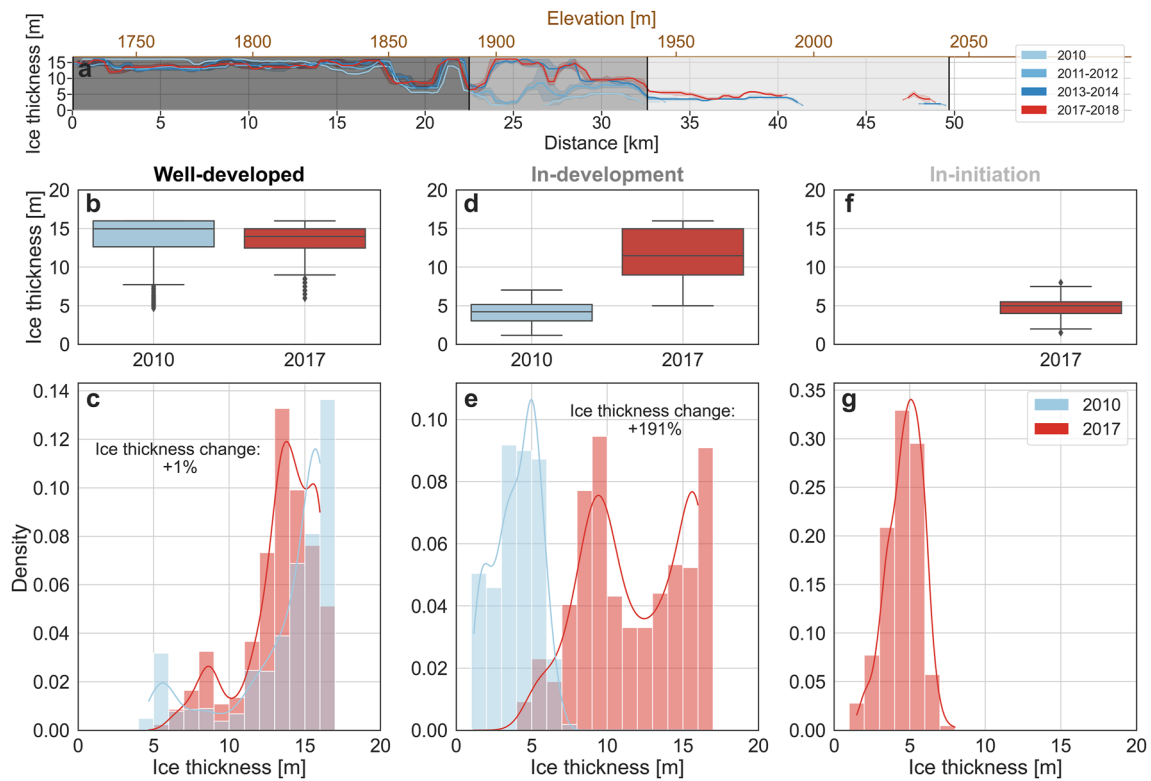


Figure 3. Ice thickness change along transect F. (a) Ice thickness change from 2010 to 2017 (colored lines). The different development stages are indicated by the background shading: well-developed (dark gray), in-development (gray), in-initiation (light gray). (b, d, f) Boxplot of ice thickness in 2010 and 2017 in the three sectors. (c, e, g) Distribution of ice thickness in 2010 and 2017 in the three sectors. Lines denote the kernel density estimate of the distributions. Percentage change indicate the relative change in total ice thickness in 2017 compared to 2010.

5.6 km there was ~4 m of thickening predominantly below the slab between 2012 and 2018 (Figures 4b and 4d). Around 1.5 m of this thickening occurred predominantly below the slab during the extreme melt summer of 2012 (Figure S5 in Supporting Information S1, 1273 °C PDH, upper quartile of 2009–2017 PDH). A further ~2.5 m of accretion during 2014–2017 was split between thickening from above and below (Figures 4c and 4d). We also observed instances of localized accretion below existing slabs in transects A, B, E, and F (Figure S8 in Supporting Information S1).

In most areas we did not see the development of “blobs” below existing slabs. The majority of accretion was relatively uniform and therefore most likely occurred on top of existing slabs. Full assessment of uniform accretion on top of slabs first requires estimation of their horizontal displacement by ice flow and vertical displacement by accumulation. In the case of transect E, the slab was displaced westward by ~52 m yr⁻¹ and downward by 0.4–0.5 m yr⁻¹ (see Text S3 in Supporting Information S1). Once we account for these displacements, from 0 to 8 km the overall offset between the apparent slab bottoms in 2012 and in 2018 is indicative of ~0.7 m firn replenishment and ~1.8 m uniform accretion on the slab top. This uniform accretion occurred alongside localized “ice blobs” forming below the slab. In the region from 6.5 to 7.7 km, which lacks any under-slab accretion, we observe 2.9 m of uniform thickening between 2012 and 2018 (Figure 4d). Further examples of accretion on top of existing ice slabs in transects C–F are shown in Figure S8 in Supporting Information S1.

At KAN_U, ice thickness change can be compared directly with in-situ estimates of melting. 0.8 m of ice accreted on top of the ice slab due to high PDH in summer 2012, approximately doubling its thickness (Figure 4b). During summer 2013 there was a further 0.6 m accretion on top of the slab (Figures 4b and 4c), even though the 2013 PDH was only 30% of the 2012 PDH. The subsequent 2.5 m of thickening between 2014 and 2018 occurred due to moderate melting in 2014 and 2016 (PDH between the median and upper quartile for 2009–2017) and limited melting in 2015 and 2017 (PDH less than the lower quartile for 2009–2017).

At higher elevations where ice slabs are in initiation, we cannot distinguish between accretion on top of versus below existing ice layers. At 2012’s upper ice slab boundary (8.5 km), a ~1 m layer grew by spring 2013,

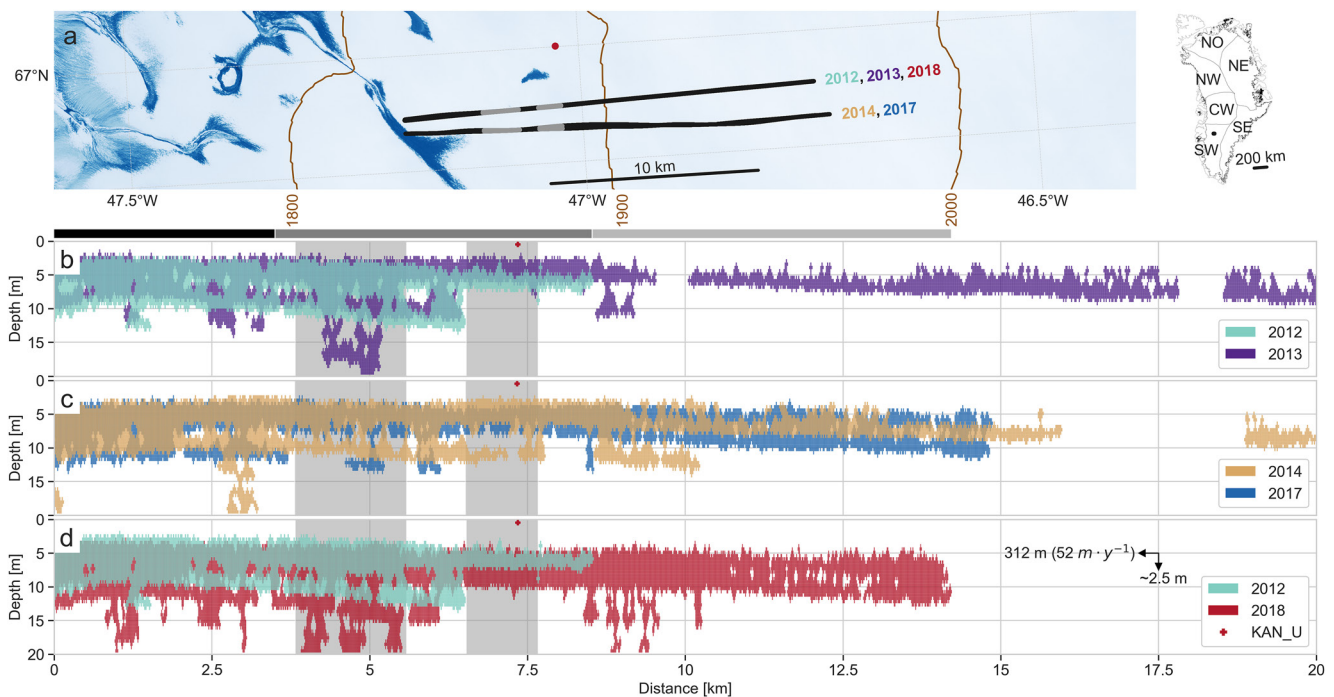


Figure 4. Ice thickness change through time close to KAN_U. (a) Near-infrared Sentinel-2 image acquired on 23 August 2021, radargram extent (black), locations where distinct accretion at depth and on the top is observed (gray), location of KAN_U (red dot). (b–d) Maximum likely ice thickness. Gray shading corresponds to panel (a). (d) the vertical arrow illustrates burial due to firn replenishment; the horizontal arrow illustrates lateral ice flow, both from 2012 to 2018 (Text S3 in Supporting Information S1). Rectangles on top of panel b–d delineate sectors of ice slabs thickness change through time (black) “well-developed” sector (dark gray) “in-development” sector (light gray) “in-initiation” sector.

subsequently thickening to 6 m by 2018 and yielding 5.7 km of inland slab expansion (Figure 4d). Conversely, from ~15 km onwards the ice layer identified in spring 2013 (Figure 4b) was buried by subsequent accumulation (Figure 4d).

4. Discussion

4.1. Mechanisms of Ice Slab Formation and Thickening

We identify three principal mechanisms of ice slab formation and thickening. (i) Meltwater percolation and refreezing generates initial ice layers in porous firn. Then, accretion of ice by meltwater refreezing proceeds (ii) on top of, and/or (iii) beneath pre-existing ice layers.

In the data presented in Figure 4, mechanism (i) was responsible for the initial generation of a 3 m-thick contiguous ice slab by the fusing of pre-existing ice layers in porous firn from 8.5 km onwards during summer 2012. Culberg et al. (2021) and de la Peña et al. (2015) similarly showed that the initiation of near-surface ice layers can occur within a single extremely warm summer.

Radar observations can often differentiate between subsequent thickening by accretion (ii) on top of, and (iii) below existing ice. We interpret that unexceptional but sustained melting conditions such as in 2014 or 2016 predominantly cause thickening by accretion on top of pre-existing ice slabs (Figure 4c). Machguth et al. (2016) also evidenced ice accretion on top of the existing ice slab due to the 2013 and 2014 moderate melt summers by comparing 2015 and 2013 cores. Hence, once ice slabs form, they thicken even in moderate melt years.

Accretion below existing ice slabs (Figures 4b and 4d) was primarily associated with the very large PDH sum during summer 2012. We propose that abundant meltwater—which may have originated from higher elevations (Clerx et al., 2022)—was able to exploit local areas of higher permeability despite the overall role of ice slabs as near-impermeable aquitards. Although previous observations show that deep percolation (>10 m) can occur in firn without homogeneous wetting front advance (Humphrey et al., 2012; Machguth et al., 2016; Samimi

et al., 2020), these processes are less likely to occur through several meters thick ice slabs. However, in north-west Greenland, Culberg et al. (2022) found that meltwater associated with visible runoff features probably exploits fractures to penetrate through the ice slab and refreeze underneath. We find multiple lines of evidence which support this process further south. First, crevasses have been observed at high elevations in the percolation zone of central-west Greenland (Colgan et al., 2016), providing paths for meltwater to flow vertically. Second, localized accretion beneath the ice slab downstream of KAN_U (Figure 4) is associated with surface meltwater ponding in a slush field (Figure S9 in Supporting Information S1). Third, sudden firn warming at 5 m depth beneath KAN_U in September 2012 strongly supports abrupt meltwater penetration through a 3 m thick ice slab, followed by gradual cooling through winter which is indicative of refreezing (Figures S4 and S5a in Machguth et al., 2016). Finally, firn cores acquired in 2012 and 2013 show ice accretion at a depth of 5 m in-between existing ice slabs (Figure S4c in Machguth et al., 2016).

4.2. Changes in Sub-Surface Firn and Implications

Immediately above the current ice slab extent in SW Greenland, the firn is primed for further ice slab development. Indeed, cores from Site J (2040 m asl) acquired in 1989 and 2017 clearly show the merging of ice lenses into several ~1 m thick layers in the uppermost 12 m (Rennermalm et al., 2021), and cores acquired at Dye-2 (2,120 m asl) in 1998 and 2013 tell a similar story (Machguth et al., 2016). The increase in firn density and ice thickness is consistent with recent warmer surface conditions (de la Peña et al., 2015).

Surface melting is projected to increase in the percolation zone (Fettweis et al., 2013; Franco et al., 2013), and extreme summer melting events such as 2010 and 2012 are expected to become more frequent (Bevis et al., 2019). Yet, radargrams indicate that the fate of the near-surface ice layer generated in summer 2012 varied by elevation.

Toward the lower elevations of the ice layer that was mostly generated due to summer 2012 (from 8.5 km onwards), additional ice accreted, forming ice slabs by 2017–2018 (Figure 4). Conversely, at higher elevations (from ~14 km onwards) where melt was infrequent between 2013 and 2017, the near-surface layer generated in 2012 was gradually buried, reducing the likelihood that it will support future ice slab growth. The upper limit of the summer 2012 ice layer identified by radar was located 260 m away from the location of Core 3 (Rennermalm et al., 2021). In 2013, this core contained numerous ice layers in the uppermost 9 m. By 2018, these ice layers had been buried and could no longer be identified by radar (Figures 4b and 4d), in agreement with ~3.5 m of firn replenishment identified by redrilling Core 3 in 2019. This is consistent with Culberg et al. (2021), who showed that the 2012 near-surface melt layer above 2,600 m asl in central Greenland was initially located at 1 m deep, and was still present in 2017 but had been buried to a depth of 5 m. Thus, the ability of near-surface ice layers to support subsequent ice slab development is likely to depend on whether strong melting occurs during several successive summers.

Considering recent sub-surface changes between 2013 and 2017, cores at KAN_U show that the top of the ice slab was at roughly the same depth in 2017 as 2013 (Figure 6a in Rennermalm et al. (2021), see also Text S3 in Supporting Information S1). However, the 2015 and 2016 cores showed some evidence of firn replenishment. We suggest that this replenishment subsequently melted during summer 2016 and refroze on top of the slab. Thus, the effect of isolated years of firn replenishment, which temporarily bury an ice slab, can be easily erased by relatively moderate melting.

5. Conclusions

We interpreted accumulation radar data to show that ice slabs already existed in 2002–2003 in SW, CW and NO Greenland, which are most likely a result of increasing surface melting from the mid-1990s onwards (van As et al., 2016). On an ice-sheet-wide basis we showed that ice slabs expanded inland from 2012 to 2018 by 13,400–17,600 km², or 37%–44%.

We identified widespread ice accretion on top of existing ice slabs and localized ice accretion beneath them. We suggest that accretion below ice slabs takes place where there is ponded surface meltwater which exploits local fractures in otherwise near-impermeable ice slabs. Accretion below ice slabs is therefore more likely during extreme melting, while more moderate melt seasons mainly result in accretion on top of existing ice.

Extremely warm summers such as 2012 can produce enough meltwater at higher elevations to fuse existing near-surface ice layers into a slab on the order of a meter thick. Once formed, ice slabs continue to thicken, even under moderate melting conditions.

We suggest that future increases in melting at higher elevations will trigger further ice slab development, increasing the ice slab area non-linearly with elevation because of the non-linearity of the hypsometry of the ice sheet (Bauer, 1955). The recent expansion of the ice sheet's visible runoff area (Tedstone & Machguth, 2022) corresponds strongly with the ice slabs extent (Figure S10 in Supporting Information S1), so future increases in ice slab area are likely to further increase the area which contributes runoff to the oceans.

Data Availability Statement

2002–2003 and 2010–2018 accumulation radar data (CReSIS, 2021) are available on the CReSIS data repository (<https://data.cresis.ku.edu/data/accum/>). We used the ArcticDEM digital elevation model at 100 m resolution, which provides elevation above the WGS84 ellipsoid (<https://www.pgc.umn.edu/data/arcticdem/>). The regional divisions of the Greenland Ice Sheet are the ones used by The IMBIE Team, (2020) and can be downloaded at <http://imbie.org/imbie-3/drainage-basins/>. Air temperatures at the automatic weather station KAN_U station can be downloaded from <https://doi.org/10.22008/promice/data/aws>. Sentinel 2 satellite images can be downloaded at <https://scihub.copernicus.eu/dhus/#/home>. The scripts used to perform the analysis for this study can be found at https://github.com/jullien/changing_Greenland_iceslabs. Our ice slab data set is available at <https://doi.org/10.5281/zenodo.7505426>.

References

- Bauer, A. (1955). The balance of the Greenland ice sheet. *Journal of Glaciology*, 2(17), 456–462. Cambridge Core. <https://doi.org/10.3189/002214355793702271>
- Bevis, M., Harig, C., Khan, S. A., Brown, A., Simons, F. J., Willis, M., et al. (2019). Accelerating changes in ice mass within Greenland, and the ice sheet's sensitivity to atmospheric forcing. *Proceedings of the National Academy of Sciences*, 116(6), 1934–1939. <https://doi.org/10.1073/pnas.1806562116>
- Braithwaite, R. J., Laternser, M., & Pfeffer, W. T. (1994). Variations of near-surface firn density in the lower accumulation area of the Greenland ice sheet, Pákitsoq, West Greenland. *Journal of Glaciology*, 40(136), 477–485. Cambridge Core. <https://doi.org/10.3189/S002214300001234X>
- Brown, J., Harper, J., Pfeffer, W. T., Humphrey, N., & Bradford, J. (2011). High-resolution study of layering within the percolation and soaked facies of the Greenland ice sheet. *Annals of Glaciology*, 52(59), 35–42. <https://doi.org/10.3189/172756411799096286>
- Carl, L., Lewis, C., Gogineni, P., Rodriguez, F., Paden, J., & Li, J. (2023). IceBridge accumulation radar L1B geolocated radar echo strength profiles, 2010, 2011, 2012, 2013, 2014, 2017, 2018. [Dataset]. Boulder, Colorado USA: National Snow and Ice Data Center. Digital media. <https://data.cresis.ku.edu/data/accum/>
- Clerx, N., Machguth, H., Tedstone, A., Jullien, N., Wever, N., Weingartner, R., & Roessler, O. (2022). In situ measurements of meltwater flow through snow and firn in the accumulation zone of the SW Greenland Ice Sheet. *The Cryosphere*, 16(10), 4379–4401. <https://doi.org/10.5194/tc-16-4379-2022>
- Colgan, W., Rajaram, H., Abdalati, W., McCutchan, C., Mottram, R., Moussavi, M. S., & Grigsby, S. (2016). Glacier crevasses: Observations, models, and mass balance implications: Glacier Crevasses. *Reviews of Geophysics*, 54(1), 119–161. <https://doi.org/10.1002/2015RG000504>
- CReSIS (2021). Accumulation radar Data, 2002, 2003, 2010, 2011, 2012, 2013, 2014, 2017, 2018. [Dataset]. Lawrence, Kansas, USA. Digital Media. <http://data.cresis.ku.edu/>
- Culberg, R., Chu, W., & Schroeder, D. M. (2022). Shallow fracture buffers high elevation runoff in northwest Greenland. *Geophysical Research Letters*, 49(23), e2022GL101151. <https://doi.org/10.1029/2022GL101151>
- Culberg, R., Schroeder, D. M., & Chu, W. (2021). Extreme melt season ice layers reduce firn permeability across Greenland. *Nature Communications*, 12(1), 2336. <https://doi.org/10.1038/s41467-021-22656-5>
- de la Peña, S., Howat, I. M., Nienow, P. W., van den Broeke, M. R., Mosley-Thompson, E., Price, S. F., et al. (2015). Changes in the firn structure of the Western Greenland Ice Sheet caused by recent warming. *The Cryosphere*, 9(3), 1203–1211. <https://doi.org/10.5194/tc-9-1203-2015>
- Enderlin, E. M., Howat, I. M., Jeong, S., Noh, M.-J., van Angelen, J. H., & van den Broeke, M. R. (2014). An improved mass budget for the Greenland ice sheet. *Geophysical Research Letters*, 41(3), 866–872. <https://doi.org/10.1002/2013GL059010>
- Fausto, R. S., van As, D., Mankoff, K. D., Vandecrux, B., Citterio, M., Ahlstrøm, A. P., et al. (2021). Programme for Monitoring of the Greenland Ice Sheet (PROMICE) automatic weather station data. *Earth System Science Data*, 13(8), 3819–3845. <https://doi.org/10.5194/essd-13-3819-2021>
- Fettweis, X., Box, J. E., Agosta, C., Amory, C., Kittel, C., Lang, C., et al. (2017). Reconstructions of the 1900–2015 Greenland ice sheet surface mass balance using the regional climate MAR model. *The Cryosphere*, 19(2), 1015–1033. <https://doi.org/10.5194/tc-11-1015-2017>
- Fettweis, X., Franco, B., Tedesco, M., van Angelen, J. H., Lenaerts, J. T. M., van den Broeke, M. R., & Gallée, H. (2013). Estimating the Greenland ice sheet surface mass balance contribution to future sea level rise using the regional atmospheric climate model MAR. *The Cryosphere*, 2(2), 469–489. <https://doi.org/10.5194/tc-7-469-2013>
- Forster, R. R., Box, J. E., van den Broeke, M. R., Miège, C., Burgess, E. W., van Angelen, J. H., et al. (2014). Extensive liquid meltwater storage in firn within the Greenland ice sheet. *Nature Geoscience*, 7(2), 95–98. <https://doi.org/10.1038/ngeo2043>
- Franco, B., Fettweis, X., & Erpicum, M. (2013). Future projections of the Greenland ice sheet energy balance driving the surface melt. *The Cryosphere*, 7(1), 1–18. <https://doi.org/10.5194/tc-7-1-2013>
- Hall, D. K., Comiso, J. C., DiGirolamo, N. E., Shuman, C. A., Box, J. E., & Koenig, L. S. (2013). Variability in the surface temperature and melt extent of the Greenland ice sheet from modis: Temperature and melt of Greenland ice. *Geophysical Research Letters*, 40(10), 2114–2120. <https://doi.org/10.1002/grl.50240>
- Harper, J., Humphrey, N., Pfeffer, W. T., Brown, J., & Fettweis, X. (2012). Greenland ice-sheet contribution to sea-level rise buffered by meltwater storage in firn. *Nature*, 491(7423), 240–243. <https://doi.org/10.1038/nature11566>
- Hock, R. (2003). Temperature index melt modelling in mountain areas. *Journal of Hydrology*, 282(1–4), 104–115. [https://doi.org/10.1016/S0022-1694\(03\)00257-9](https://doi.org/10.1016/S0022-1694(03)00257-9)

- Humphrey, N. F., Harper, J. T., & Pfeffer, W. T. (2012). Thermal tracking of meltwater retention in Greenland's accumulation area: Thermal tracking of meltwater retention. *Journal of Geophysical Research*, *117*(F1), F01010. <https://doi.org/10.1029/2011JF002083>
- Kanagaratnam, P., Gogineni, S. P., Ramasami, V., & Braaten, D. (2004). A wideband radar for high-resolution mapping of near-surface internal layers in glacial ice. *IEEE Transactions on Geoscience and Remote Sensing*, *42*(3), 483–490. <https://doi.org/10.1109/TGRS.2004.823451>
- King, M. D., Howat, I. M., Candela, S. G., Noh, M. J., Jeong, S., Noël, B. P. Y., et al. (2020). Dynamic ice loss from the Greenland Ice Sheet driven by sustained glacier retreat. *Communications Earth & Environment*, *1*(1), 1. <https://doi.org/10.1038/s43247-020-0001-2>
- Lewis, C. (2010). *Airborne UHF radar for fine resolution mapping of near-surface accumulation layers in Greenland and west Antarctica*. (Master's thesis). [University of Kansas]. Retrieved from KU Scholar Works data repository Retrieved from <http://hdl.handle.net/1808/7008>
- MacFerrin, M., Machguth, H., van As, D., Charalampidis, C., Stevens, C. M., Heilig, A., et al. (2019). Rapid expansion of Greenland's low-permeability ice slabs. *Nature*, *573*(7774), 403–407. <https://doi.org/10.1038/s41586-019-1550-3>
- Machguth, H., MacFerrin, M., van As, D., Box, J. E., Charalampidis, C., Colgan, W., et al. (2016). Greenland meltwater storage in firn limited by near-surface ice formation. *Nature Climate Change*, *6*(4), 390–393. <https://doi.org/10.1038/nclimate2899>
- Miège, C., Forster, R. R., Brucker, L., Koenig, L. S., Solomon, D. K., Paden, J. D., et al. (2016). Spatial extent and temporal variability of Greenland firn aquifers detected by ground and airborne radars. *Journal of Geophysical Research: Earth Surface*, *121*(12), 2381–2398. <https://doi.org/10.1002/2016JF003869>
- Mikkelsen, A. B., Hubbard, A., MacFerrin, M., Box, J. E., Doyle, S. H., Fitzpatrick, A., et al. (2016). Extraordinary runoff from the Greenland ice sheet in 2012 amplified by hypsometry and depleted firn retention. *The Cryosphere*, *10*(3), 1147–1159. <https://doi.org/10.5194/tc-10-1147-2016>
- Miller, J. Z., Culberg, R., Long, D. G., Shuman, C. A., Schroeder, D. M., & Brodzik, M. J. (2022). An empirical algorithm to map perennial firn aquifers and ice slabs within the Greenland Ice Sheet using satellite L-band microwave radiometry. *The Cryosphere*, *16*(1), 103–125. <https://doi.org/10.5194/tc-16-103-2022>
- Nghiem, S. V., Hall, D. K., Mote, T. L., Tedesco, M., Albert, M. R., Keegan, K., et al. (2012). The extreme melt across the Greenland ice sheet in 2012. *Geophysical Research Letters*, *39*(20), 2012GL053611. <https://doi.org/10.1029/2012GL053611>
- Pfeffer, W. T., & Humphrey, N. F. (1998). Formation of ice layers by infiltration and refreezing of meltwater. *Annals of Glaciology*, *26*, 83–91. <https://doi.org/10.3189/1998AoG26-1-83-91>
- Pfeffer, W. T., Meier, M. F., & Illangasekare, T. H. (1991). Retention of Greenland runoff by refreezing: Implications for projected future sea level change. *Journal of Geophysical Research*, *96*(C12), 22117. <https://doi.org/10.1029/91JC02502>
- Rennermalm, Å. K., Hock, R., Covi, F., Xiao, J., Corti, G., Kingslake, J., et al. (2021). Shallow firn cores 1989–2019 in southwest Greenland's percolation zone reveal decreasing density and ice layer thickness after 2012. *Journal of Glaciology*, *68*(269), 431–442. <https://doi.org/10.1017/jog.2021.102>
- Rignot, E., Box, J. E., Burgess, E., & Hanna, E. (2008). Mass balance of the Greenland ice sheet from 1958 to 2007. *Geophysical Research Letters*, *35*(20), L20502. <https://doi.org/10.1029/2008GL035417>
- Rodriguez-Morales, F., Byers, K., Crowe, R., Player, K., Hale, R. D., Arnold, E. J., et al. (2014). Advanced multifrequency radar instrumentation for polar Research. *IEEE Transactions on Geoscience and Remote Sensing*, *52*(5), 2824–2842. <https://doi.org/10.1109/TGRS.2013.2266415>
- Rodriguez-Morales, F., Gogineni, P., Leuschen, C., Allen, C., Lewis, C., Patel, A., et al. (2010). Development of a multi-frequency airborne radar instrumentation package for ice sheet mapping and imaging. In *2010 IEEE MTT-S international microwave symposium* (pp. 157–160). <https://doi.org/10.1109/MWSYM.2010.5518197>
- Samimi, S., Marshall, S. J., & MacFerrin, M. (2020). Meltwater penetration through temperate ice layers in the percolation zone at DYE-2, Greenland ice sheet. *Geophysical Research Letters*, *47*(15), e2020GL089211. <https://doi.org/10.1029/2020GL089211>
- Tedesco, M., & Fettweis, X. (2020). Unprecedented atmospheric conditions (1948–2019) drive the 2019 exceptional melting season over the Greenland ice sheet. *The Cryosphere*, *14*(4), 1209–1223. <https://doi.org/10.5194/tc-14-1209-2020>
- Tedesco, M., Fettweis, X., Mote, T., Wahr, J., Alexander, P., Box, J. E., & Wouters, B. (2013). Evidence and analysis of 2012 Greenland records from spaceborne observations, a regional climate model and reanalysis data. *The Cryosphere*, *7*(2), 615–630. <https://doi.org/10.5194/tc-7-615-2013>
- Tedesco, M., Fettweis, X., van den Broeke, M. R., van de Wal, R. S. W., Smeets, C. J. P. P., van de Berg, W. J., et al. (2011). The role of albedo and accumulation in the 2010 melting record in Greenland. *Environmental Research Letters*, *6*(1), 014005. <https://doi.org/10.1088/1748-9326/6/1/014005>
- Tedstone, A. J., & Machguth, H. (2022). Increasing surface runoff from Greenland's firn areas. *Nature Climate Change*, *12*(7), 672–676. <https://doi.org/10.1038/s41558-022-01371-z>
- The IMBIE Team. (2020). Mass balance of the Greenland ice sheet from 1992 to 2018. *Nature*, *579*(7798), 233–239. <https://doi.org/10.1038/s41586-019-1855-2>
- van den Broeke, M. R., Enderlin, E. M., Howat, I. M., Kuipers Munneke, P., Noël, B. P. Y., van de Berg, W. J., et al. (2016). On the recent contribution of the Greenland ice sheet to sea level change. *The Cryosphere*, *10*(5), 1933–1946. <https://doi.org/10.5194/tc-10-1933-2016>
- van Angelen, J. H., van den Broeke, M. R., Wouters, B., & Lenaerts, J. T. M. (2014). Contemporary (1960–2012) evolution of the climate and surface mass balance of the Greenland ice sheet. *Surveys in Geophysics*, *35*(5), 1155–1174. <https://doi.org/10.1007/s10712-013-9261-z>
- van As, D., Fausto, R. S., Cappelen, J., van de Wa, R. S. W. I., Braithwaite, R. J., Machguth, H., & Promice project team. * (2016). Placing Greenland ice sheet ablation measurements in a multi-decadal context. *GEUS Bulletin*, *35*, 71–74. <https://doi.org/10.34194/geusb.v35.4942>
- Vandecrux, B., MacFerrin, M., Machguth, H., Colgan, W. T., van As, D., Heilig, A., et al. (2019). Firn data compilation reveals widespread decrease of firn air content in Western Greenland. *The Cryosphere*, *13*(3), 845–859. <https://doi.org/10.5194/tc-13-845-2019>

References From the Supporting Information

- Doyle, S. H., Hubbard, A., Fitzpatrick, A. A., Van As, D., Mikkelsen, A. B., Petterson, R., & Hubbard, B. (2014). Persistent flow acceleration within the interior of the Greenland ice sheet. *Geophysical Research Letters*, *41*(3), 899–905. <https://doi.org/10.1002/2013GL058933>
- Fettweis, X., Hofer, S., Krebs-Kanzow, U., Amory, C., Aoki, T., Berends, C. J., et al. (2020). GrSMBMIP: Intercomparison of the modelled 1980–2012 surface mass balance over the Greenland ice sheet. *The Cryosphere*, *24*(11), 3935–3958. <https://doi.org/10.5194/tc-14-3935-2020>
- Karlsson, N. B., Colgan, W. T., Binder, D., Machguth, H., Abermann, J., Hansen, K., & Pedersen, A. Ø. (2019). Ice-penetrating radar survey of the subsurface debris field at Camp Century, Greenland. *Cold Regions Science and Technology*, *165*, 102788. <https://doi.org/10.1016/j.coldregions.2019.102788>